Theoretical and Applied Climatology (2021) 146:71–90
https://doi.org/10.1007/s00704-021-03721-x

ORIGINAL PAPER

Decadal changes of heatwave aspects and heat index over Egypt

Mostafa Morsy[1] · **Gamal El Afandi**[1,2]

Received: 19 September 2020 / Accepted: 2 July 2021 / Published online: 22 July 2021

Abstract
This study aims to utilize the existing new and superior heatwave (HW) indices (ClimPACTv2) software to identify the decadal changes of HW aspects (number (HWN), duration (HWD), frequency (HWF), amplitude (HWA), and magnitude (HWM)) over Egypt during the period 1979–2018. The 90th percentile threshold maximum (TX90), minimum (TN90) temperatures, and excess heat factor (EHF) indices were chosen to compute these five HW aspects. The results showed that the lowest decadal summations of HWN (5–20), HWD (20–40 days), and HWF (20–80 days) were detected in the first decade (1979–1988) and increased significantly with positive decadal anomaly trends up to the last decade (2009–2018). Furthermore, Egypt especially the southeastern part subjected to HWA above 300 °C and HWM above 200 °C from both TX90 and TN90 and is confined to the northwestern part with HWA above 140°C^2 and HWM exceed 50°C^2 from EHF, particularly during the last two decades. Also, the decadal averages of temperature (T, °C) increased gradually over time especially in the southeastern part of Egypt, while the decadal averages of relative humidity (RH, %) nearly remained constant. Therefore, T has a most effective role than RH in determining HI over Egypt during the study period. This creates a relatively tolerable environment for the human body despite the increasing trend over time in the five HW aspects. Thus, all of Egypt falls within the heat index (HI) caution range (26–32 °C) except for the southeastern part which has extreme caution values (32–41 °C) in the last two decades.

1 Introduction

Extreme temperature (heatwave) represents one of the most significant climate features, natural hazards, and extreme weather events. It could cause a high number of casualties and threaten different sectors, especially the developing countries (Piticar et al. 2018). This includes agriculture, ecosystems, transportation, energy, water resources, environment, infrastructure, human health, and other living organisms in large parts of the world (Abatan et al. 2016; Andersen et al. 2005; Añel et al. 2017; Barriopedro et al. 2011; Coumou and Rahmstorf 2012; Dole et al. 2011; Fink et al. 2004; Lesk et al. 2016; Stott et al. 2004; Koppe et al. 2004; WHO 2010; Zampieri et al. 2016). In addition, it causes more deaths than any other extreme weather event all over the world (Shaposhnikov et al. 2014; Nairn and Fawcett 2015; Kim et al. 2016; Chen et al. 2017). IPCC (2013) has revealed that there is a rising trend in the global mean surface air temperature over the last 100 years, as well as heatwaves (HWs), which occur with a higher frequency, intensity, and length if there is an increase in the greenhouse gas concentrations. Furthermore, some previous climate studies in different regions of the globe (e.g., Perkins et al. 2012; Fontaine et al. 2013; Spinoni et al. 2015; Wang et al. 2016) have shown that there is a significant increase in HW number, frequency, intensity, and duration. In the context of the projected global warming and climate variability, many research studies (regional and global scale) proposed that the frequency and intensity of hot extremes will be increased in the future decades (Fischer and Schär 2010; Sillmann et al. 2013; Russo et al. 2014; Lelieveld et al. 2016).

The Middle East and North Africa (MENA) region are expected to be strongly influenced by global climate warming, increasing the already dry and hot environmental conditions (Önol et al. 2014; Ozturk et al. 2015). Long-term temperature analysis in the eastern Mediterranean and Middle East region suggests that since the 1970s, the frequency and number of heat extremes (waves) have increased (Tanarhte et al. 2015). HWs and extreme

✉ Mostafa Morsy
mostafa_morsy@azhar.edu.eg

[1] Astronomy and Meteorology Department, Faculty of Science, Al-Azhar University, Cairo 11884, Egypt

[2] College of Agriculture, Environment and Nutrition Sciences, Tuskegee University, Tuskegee, AL 36088, USA

temperature trends in the eastern Mediterranean region have been assessed by Kuglitsch et al. (2010) and Kostopoulou et al. (2014). The summer season was found to have the most significant extreme temperature trends, where both maximum and minimum temperature extremes demonstrate statistically significant warming trends (Kostopoulou and Jones 2005). The trend analysis of temperature extremes in the Mediterranean region, based on daily gridded temperature data sets since the mid-twentieth century, shows a decrease in cold extremes and an increase in hot extremes (Efthymiadis et al. 2011). Also, the number, duration, and intensity of HWs in the eastern Mediterranean increased (Kuglitsch et al. 2010). Furthermore, the southern and southeastern parts of Turkey have a significant warming trend for the period 1950–2004 (Tayanç et al. 2009). Based on 97 meteorological stations for the period 1950–2010 in Turkey, Erlat and Türkes (2013) showed that there has been an upward trend in the annual number of summer and tropical days. Zhang et al. (2005) have assessed the variation in extreme temperature and precipitation at 52 stations from 15 countries in the Middle East for the period 1950–2003. Their results revealed an upward trend in the annual maximum and frequency of daily maximum where the daily temperature has exceeded its 90th percentile. Donat et al. (2014) found that the frequency of both warm days and nights has been increased, as well as higher extreme temperature values in the Arab region. Athar (2014) showed that temperature extremes display warmer in the summer season along with the southwest coastal stations, indicating more warming, compared to the inland stations, based on observed daily temperature datasets for a 30-year period (1979–2008) at 19 stations in Saudi Arabia. Kousari et al. (2013) found positive trends of monthly, seasonal, and annual maximum temperature in the warm seasons of the climatic period of 1960–2005 for 32 stations in Iran with a significant upward trend after 1970. Analysis of the temperature trend from seven stations in Iraq during the period 1941–2013 revealed that trends with the strongest warming trends in the summer season are generally increasing (Muslih and Błażejczyk 2017). From previous research, it is clear that HWs are expected not only to become more frequent but also to become more severe (Alghamdi and Harrington 2018).

Climatological studies of HWs and extreme temperatures in Egypt were based only on one HW and its associated atmospheric circulation and synoptic situations (Hasanean 2004; Abdel Basset and Hasanen 2006). The variation of summer temperature over Egypt has been studied using 19 stations for different periods up to 2000 (Hasanean and Abdel Basset 2006). Their trend analysis of the time series of the selected stations showed remarkable positive (increase) trend values during the last 20 years. The number of hot days with maximum temperature exceeds the 90th percentile at three weather stations in Egypt was applied to calculate short HWs (3 to 6 consecutive days) and long HWs (6 or more consecutive days) have been investigated by El Ashmawy (2015). His study showed a significant increase in hot days and HWs with time, particularly in the period 1991–2010. In addition, Saleh et al. (2017) studied the HW events and their impact on wheat and maize production in 3 governorates in different climatic regions in Egypt (Behira, Giza, and Qena governorates representing North Delta, Middle Egypt, and Upper Egypt respectively) during the period 1980–2015. They found that the highest monthly maximum temperature, which was noticed in the summer season, was in August 2015 followed by August 2012 (reduced maize productivity), while the highest extreme HWs were recorded in the winter season of 2010 (reduced wheat productivity). Domroes and El-Tantaw (2005) applied a principal component analysis to compute temperature trends across Egypt based on 6 and 9 stations for the period 1941–2000 and 1971–2000 respectively. Analysis of observations in the period 1941–2000 indicates that decreasing trends were found in the mean annual and maximum temperatures and seasonally in autumn and winter while increasing trends were shown in the mean minimum temperature and seasonally in the spring and summer. From the period 1971–2000, positive trends prevailed for all seasons and temperatures except for maximum temperature. Khalil and Hassanein (2016) investigated and identified the impacts of three extreme weather events (extreme heat and cold temperatures, extreme wind, and extreme precipitation) on agriculture at 12 weather stations in Egypt during 1990–2015. Their results indicated that the duration and frequency of extreme weather events and the hotter and colder waves in Egypt have been increased in recent past years and affected different crops. The spatial patterns in annual and seasonal temperature, rainfall, and related extremes trends in Egypt have been assessed using a modified Mann-Kendal trend test by Nashwan et al. (2018). The daily rainfall and temperature data (1948–2010) of the Princeton Global Meteorological Forcing with a spatial resolution of $0.25° \times 0.25°$ were used for this purpose. The Mann-Kendal test showed upward trends in temperature and several temperature extremes in Egypt but almost no change in rainfall and rainfall extremes. At the same time, the minimum temperature was found to increase much faster compared to the maximum one and thus decrease the diurnal temperature range in most parts of Egypt. In addition, in winter, the number of hot days and nights has increased, while the cold days have been decreased in most parts of the country. Gamal (2017) has investigated future trends of extreme temperature indices for 9 stations located in the

Sinai Peninsula, Egypt, for the period 2016–2050 based on the daily future projection scenarios RCP45 and RCP85. His results demonstrated that the RCP45 scenario showed that all stations have a significant positive trend for maximum and minimum temperature exceeds their 90th percentile, also have a significant negative trend for maximum and minimum temperature below their 10^{th} percentile, whereas the results from the RCP85 scenario are the same for RCP45 but have large slopes for all trends. Said et al. (2012) focused on the changes in extreme temperature, precipitation, and sea-level events over the Alexandria region during the period 1979–2011. Their results indicated that the mean annual air temperature has increased by 2.24 °C during the study period with a rate of about 0.6 °C/decade. Air temperature, time series at three stations (Alexandria (1900–2010), Port Said (1900–1947), and Cairo (1957–2010)) of Nile Delta, Egypt, has been statistically analyzed by Hussein and Mohamed (2016). The results revealed that the highest seasonal warming trends were observed for summer temperatures and increasing temperature trends indicated with different magnitude in the rest seasons. The highest seasonal warming trend for all seasons has been recorded in Cairo compared to the other two stations.

On the other hand, to measure the effect of extreme temperatures or heatwaves on the human body and health, the influence of relative humidity and temperature is often combined to produce a heat index (HI) that expresses a human's feeling of comfort or discomfort for the ambient weather conditions. HI was originally developed by Steadman (1979) which requires the solution of multiple variables within multiple equations represented by the body's heat and moisture transfer that cannot be easily obtained. Therefore, Rothfusz (1990) performed a polynomial multiple regression analysis on Steadman's tabulated HI data and developed a simplified National Weather Service (NWS) HI equation that is mainly based on air temperature and relative humidity.

However, no comprehensive studies concerning the temporal and spatial variation of HWs and HI covering the whole territory of Egypt for long periods and homogeneous, as much as possible, were carried out. Thus, this study aims to utilize the existing new and superior approach and the NWS's HI to determine the spatial patterns and anomalies of the decadal variation in HWs and HI during the longest possible period of 1979–2018.

2 Heatwaves definitions, aspects, and indices

A period of consecutive days in which the prevailing temperature (daytime and/or night time) and thermal conditions exceed their normality is the general HWs definition (Alghamdi and Harrington 2018). HWs are an area of interest to many sectors (e.g., health, agriculture, energy, climate, and environment) and have a geographic relativism; a wide range of HW definitions and indices have been developed scientifically (Souch and Grimmond 2004). Therefore, there is no universal or identical HW definition, method, or index that works for all applications (Smith et al. 2013; Kent et al. 2014). The World Meteorological Organization (WMO) defined HW as when the daily maximum temperature of more than five consecutive days exceeds the average (normal) maximum temperature by 5 °C. Klein Tank and Konnen (2003) and Baldi et al. (2006) stated that a HW (coldwave) occurs when the temperature exceeds the 90th (below the 10th) percentile for 6 or more consecutive days of a long heatwave and 3–6 days for a short heatwave. According to Smith et al. (2013), three aspects for HWs should be determined appropriately: (a) the relevant meteorological variables (e.g., maximum temperature alone or plus one or more parameters); (b) the type of the relevant threshold (percentile or absolute) value; and (c) the duration (consecutive days). The thresholds are employed to dissect the daily maximum temperature time series, such that a HW will only found if some threshold criteria are met across a daily time window (Perkins and Alexander 2013). So, selecting the appropriate threshold, timescale (monthly, seasonally, or annually), and the period of analysis (decadal or climate) become vital and critical issues (Alghamdi and Harrington 2018). Finally, the maximum temperature is the common meteorological metric used in his assessment, but it is often combined with minimum temperature to further intensify the impact of weather conditions and HWs (Perkins and Alexander 2013). Fischer and Schar (2010) suggested a structure for studying some additional HW elements besides the duration and frequency. This structure involves the number of HW events (HWN), their duration (HWD), their frequency (HWF), and their amplitude (HWA). And, Perkins and Alexander (2013) study included the HW magnitude (HWM). These five elements are known as HW aspects as illustrated in Table 1 and usually calculated as yearly values over a climatic period (30-year time slices).

On the other hand, there are several HW indices developed by different communities and researchers that serve different applications around the world. The UTCI (Universal Thermal Climate Index) is a thermal comfort indicator, which measures the thermal stress induced by the atmospheric environment on the human body. Heat and Cold Wave Index (HCWI) is used for identifying, detecting, and characterizing the periods of extreme temperature anomalies (either heat or cold waves). Global heatwave and warm spell toolbox (GHWT) is a user-friendly and flexible toolbox developed in MATLAB to construct long-term heatwave and warm spell records with any gridded global daily temperature data source for any country around the globe (https://github.com/mojtabasadegh/Global_Heatwave_and_Warm_

Table 1 Heatwave (HWs) aspects description and units

HW aspect	Meaning	Units
HWN	The yearly number of HW events	Events
HWD	The length in days of the longest yearly HW event defined by HWN	Days
HWF	The sum of days per year that contribute to HW events defined by HWN	Days
HWA	The hottest day (or the peak daily temperature) of the hottest yearly HW	°C
HWM	The average daily magnitude for all HW events within a year	°C

Spell_Toolbox). Excess heat factor (ehfheatwaves) tool is used to calculate HWs from gridded daily datasets (https://github.com/tammasloughran/ehfheatwaves). The Expert Team on Climate Change Detection and Indices (ETCCDI) developed a set of 27 descriptive climate change indices (http://etccdi.pacificclimate.org/list_27_indices.shtml) aimed at detecting changes in moderate extremes (Mcgree et al. 2019). Due to some facts that many of the ETCCDI indices have no obvious sector relevance, some of them are based on absolute thresholds which are not suitable in some regions (Perkins 2011) and do not provide enough details for all HWs aspects (Perkins and Alexander 2013), the WMO Commission for Climatology (CCl) set up the Expert Team on Sector-Specific Climate Indices (ET-SCI). In collaboration with experts in different sectors (agricultural meteorology, water resources, and health), the ET-SCI identified and evaluated additional sector-specific (34) indices. The ET-SCI developed ClimPACTv2 (R-based) software to compute the cores set of their defined climate-related indices and it should be applied to the homogenized data series (Alexander and Herold 2015).

3 Study area and its climatic features

Egypt connects between the two African and Asian continents through the Sinai Peninsula, where it lies in the northeastern corner of the African continent and the southeastern corner of the Mediterranean Sea. The country is bounded to the north by the Mediterranean Sea, Sudan to the South, Libya to the West, Gaza Strip, Gulf of Aqaba, and the Red Sea to the East. It is astronautically extending between latitudes from 22° N to about 32° N and longitudes from 24° E to about 37° E, as shown in Fig. 1. Due to its geographical location, it is exposed to various weather systems and climatic features throughout the seasons (Aboelkhair et al. 2019). The Mediterranean climate is the dominant system in the northern part of Egypt and gradually changes to be nearly semi-desert and desert climate in its southern part (El Afandi et al. 2013). The descending motion from a branch of Hadley cell and the presence of the sub-tropical high pressure in the lower troposphere produces high static stability conditions and causes heatwaves during the summer season (June–August) over the eastern Mediterranean including Egypt (Lasheen 2000).

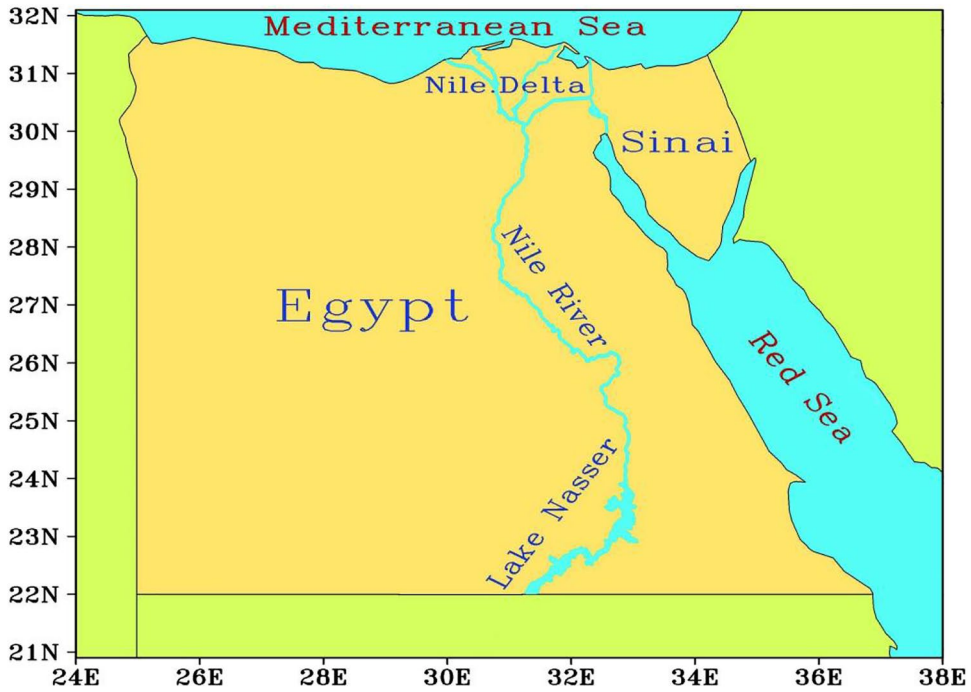

Fig. 1 Boundaries and features of the study area (shaded in yellow)

Furthermore, the Hadley cell descending motion and the horizontal advection of warm and humid air masses from the tropical areas of Indian monsoon low make adiabatic warming in the surface and lower layer in the troposphere in this region (El Ashmawy 2015). The prevailing pressure system affecting Egypt during the summer season is the westward extension of the Indian monsoon low (thermal shallow low acting over southwest Asia), which supplies a hot and humid northeasterly surface wind over Egypt. This extension of the Indian monsoon low acts as a swim with the sub-tropical high pressure; i.e., when the Indian monsoon low weakened and retarded eastward, the sub-tropical high pressure enters to invade the area. This sub-tropical high pressure is centered over western Europe and extends eastward to reach and cover the eastern Mediterranean Sea which provide a rather mild and dry north-westerly wind over the northern parts of Egypt (Abdel Basset and Hasanen 2006; El Ashmawy 2015). The analysis of the spatial distribution of the annual average of daily maximum and minimum temperature over Egypt demonstrated that temperature increases gradually towards the hot desert in the south, where the maximum and minimum temperature ranges from 22.3 to 35.0 and 10.0 to 22.5 °C respectively across Egypt (Nashwan et al. 2018).

4 Data used

Daily gridded 0.5° × 0.5° reanalysis dataset for near-surface maximum temperature (TX) °C, minimum temperature (TN) °C, and total precipitation (TP) mm for 40 years, from 01 January 1979 to 31 December 2018, was extracted over Egypt from the European Centre for Medium-Range Weather Forecasts Interim (Dee et al. 2011) dataset archive (ECMWF/ERA-Interim) server (https://apps.ecmwf.int/datasets/data/interim-full-daily/levtype=sfc/). This 0.5° × 0.5° horizontal resolution is used in this study due to computational constraints. These selected data will be used to illustrate the changes in decadal spatial distributions, trend analysis, and anomalies of HWs over Egypt during the selected four consecutive decades (1979–1988, 1989–1998, 1999–2008, and 2009–2018). The majority of available weather stations in Egypt, like most developing countries, is sparse over time and space (El Kenawy et al. 2019a) and have a degree of uncertainty since the majority of these stations is situated near the urban settlements, like airports, around the River Nile and along the coasts of both the Mediterranean and Red Sea (Peterson et al. 1998). These areas represent less than 10% of Egypt's total area, making the current meteorological network stations inadequate to properly understand and diagnose the climatology and spatio-temporal variability of heatwaves across Egypt. Therefore, the use of reanalysis meteorological datasets like ERA-Interim opens up interesting possibilities for overcoming the current limitations of ground-based meteorological measurements (El Kenawy et al. 2019b).

5 Methodology

The R package (ClimPACTv2) software is used in the present study to calculate all ET-SCI climate indices, which aims to study the five selected aspects of HWs in Egypt. Before index computations using the ClimPACTv2 software, it is necessary to check the input daily data using quality control and homogeneity that required for the robust analysis of climate time series. For the model gridded reanalysis (like ERA-Interim) datasets, there is no need to apply the quality control or homogeneity as there are no missing values overall time series (Ragatoa et al. 2019). ERA-Interim data has been retrieved in a gridded netCDF file format to be compatible with the desired ClimPACTv2 inputs, which in turn produces a netCDF file format.

Several interesting studies in the analysis of HWs in different global climatic regions used the percentile (80th, 85th, 90th, and 95th)-based indices of maximum (TX) and minimum (TN) temperatures. Along with the TX and TN percentile indices, the excess heat factor (EHF) has also been applied to quantify HWs duration and severity. The EHF was developed by Nairn et al. (2009) in the Bureau of Meteorology, Australia, and has been enhanced by Perkins and Alexander (2013) and by Nairn and Fawcett (2013). EHF is a combination of two excess heat indices of significance (EHIsig) and acclimatization (EHIacc) as in Eq. 1.

$$\mathrm{EHF} = \max[1, \mathrm{EHI}_{\mathrm{acc}}] \times \mathrm{EHI}_{\mathrm{sig}} \quad (1)$$

Table 2 Heat index severity categories and its effect on the human body based on according to the U.S. NWS

Classification	HI (°C)	Effect on the body
Caution	26–32	Fatigue possible with prolonged exposure and/or physical activity
Extreme caution	32–41	Heatstroke, heat cramps, or heat exhaustion possible with prolonged exposure and/or physical activity
Danger	41–54	Heat cramps or heat exhaustion likely and heat stroke possible with prolonged exposure and/or physical activity
Extreme danger	> 54	Heatstroke highly likely

Source: NWS website (https://www.weather.gov/ama/heatindex)

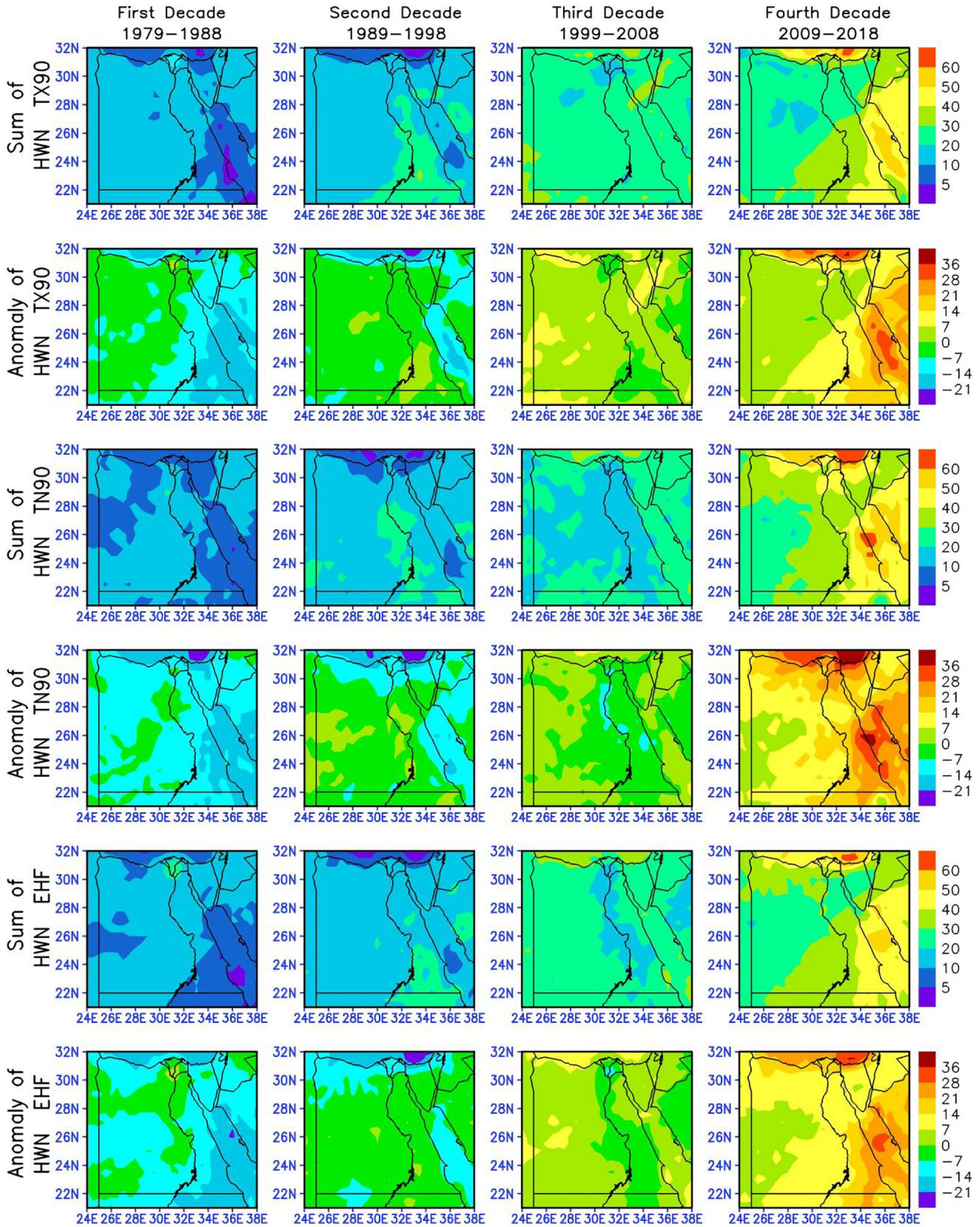

Fig. 2 Decadal summation of the yearly heatwave number (HWN) using TX90 (first row), TN90 (third row), and EHF (fifth row) with their anomalies (TX90 in the second row, TN90 in the fourth row, and EHF in the sixth row) from the average of their summation through the four decades

Table 3 The ranges of the decadal summations and anomalies of the yearly heatwave number (HWN) for each decade using the three HW definitions (TX90, TN90, and EHF)

HWN						
Decade	Decadal summation			Anomaly		
	TX90	TN90	EHF	TX90	TN90	EHF
1979–1988	2:22	4:22	4:26	− 20:0	− 24: − 2	− 20:2
1989–1998	3:30	3:30	2:26	− 21:3	− 24:6	− 24:0
1999–2008	16:36	9:39	12:36	− 6:12	− 10:12	− 10:12
2009–2018	15:65	20:75	20:65	0:35	5:45	5:35

$$EHI_{acc} = [(TM_i + TM_{i-1} + TM_{i-2})/3] - [(TM_{i-3} + \cdots + TM_{i-32})/30] \quad (2)$$

$$EHI_{sig} = [(TM_i + TM_{i-1} + TM_{i-2})/3] - TM95 \quad (3)$$

Some slight modifications in EHF_{sig} (Perkins personal comms 2015) by employing the 90th percentile-based indices instead of the 95th percentile of TM over the base period as in Eq. (4).

$$EHI_{sig} = [(TM_i + TM_{i-1} + TM_{i-2})/3] - TM90 \quad (4)$$

where TM_i is the average daily temperature for the day *i* and TM95 (TM90) is the 95th (90th) percentile of TM which is calculated via TM = (TX + TN)/2 within a user-specified base period over the calendar year and using a 15-day running window. Also, EHI_{acc} represents the anomaly over a 3-day window against the preceding 30 days and EHI_{sig} represents the anomaly of the same 3-day window against an extreme threshold (95th or 90th percentile). The EHF unit is ($°C^2$) due to multiplying the EHI_{acc} (°C) and EHI_{sig} (°C) indices (Perkins and Alexander 2013). When ClimPACTv2 is running using a netCDF dataset, the alternative version of the EHF (95th or 90th percentile) could be specified.

In this study, three HW definitions (indices) of TX > 90th percentile (TX90), TN > 90th percentile (TN90), and EHF based on the 90th percentile of TM are selected from ClimPACTv2 to identify the HW severity over Egypt using five HW aspects, where, in ClimPACTv2, the HW is defined as 3 or more consecutive days that occur each summer (November-March in southern hemisphere and May–September in northern hemisphere), where either the EHF is positive, TX > TX90 or TN > TN90. The study considered 30 years as a base (reference) period of 1981–2010 to calculate the three HW definitions (TX90, TN90, and EHF). Furthermore, the decadal HW aspect (HWN, HWD, HWF, HWA, and HWM) for the three HW definitions is calculated as the summation of the yearly aspect value in each decade (1979–1988, 1989–1998, 1999–2008, and 2009–2018), while the decadal anomalies are defined as the decadal HW aspect subtracted from the mean of the four decades summation of all aspects of three heatwave definitions. Moreover, the decadal averages and anomalies were computed for the annual averages of the monthly temperature (T, °C), relative humidity (RH, %), wind speed (WS, m/s), and heat index (HI, °C) during the summer period (May to September) of the Northern Hemisphere (as in HW aspects calculations). In addition, the time-latitudinal cross-section was applied to determine the yearly variations, latitudinal oscillations (different climatic zones), and trends in the HW aspect and HI characteristics along with the selected period 1979–2018 in Egypt. The time-latitudinal cross-section is computed as a yearly summation of the interest HW aspect and yearly average of T, RH, WS, and HI at all longitudinal grid points on each single latitudinal grid point across the whole period.

The calculation of HI is performed using the developed multiple regression by Rothfusz (1990) which is described by the NWS Technical Attachment (SR 90–23). The derived HI regression equation is:

$$\begin{aligned} HI = &((-42.379 + 2.04901523 \times T + 10.14333127 \times \\ &RH - 0.22475541 \times T \times RH - 0.00683783 \\ &\times T^2 - 0.05481717 \times RH^2 + 0.00122874 \\ &\times T^2 \times RH + 0.00085282 \times T \times RH^2 \\ &- 0.00000199 \times T^2 \times RH^2) - 32) \times 5/9 \end{aligned} \quad (5)$$

where T is the air temperature in degree Fahrenheit (°F), RH is relative humidity (%), and HI is the heat index expressed as an apparent temperature in degrees Celsius (°C). If the RH < 13% and 44.5 °C < T > 26.5 °C, then the following adjustment is subtracted from HI:

$$\text{Adjustment}(1) = \left(\frac{13 - RH}{4}\right) \times \text{SQRT}\left(\frac{17 - \text{ABS}(T - 95)}{17}\right) \quad (6)$$

where SQRT is the square root function and ABS is the absolute value. On the other hand, if the RH > 85% and 30.5 °C < T > 26.5 °C, then the following adjustment is added to HI:

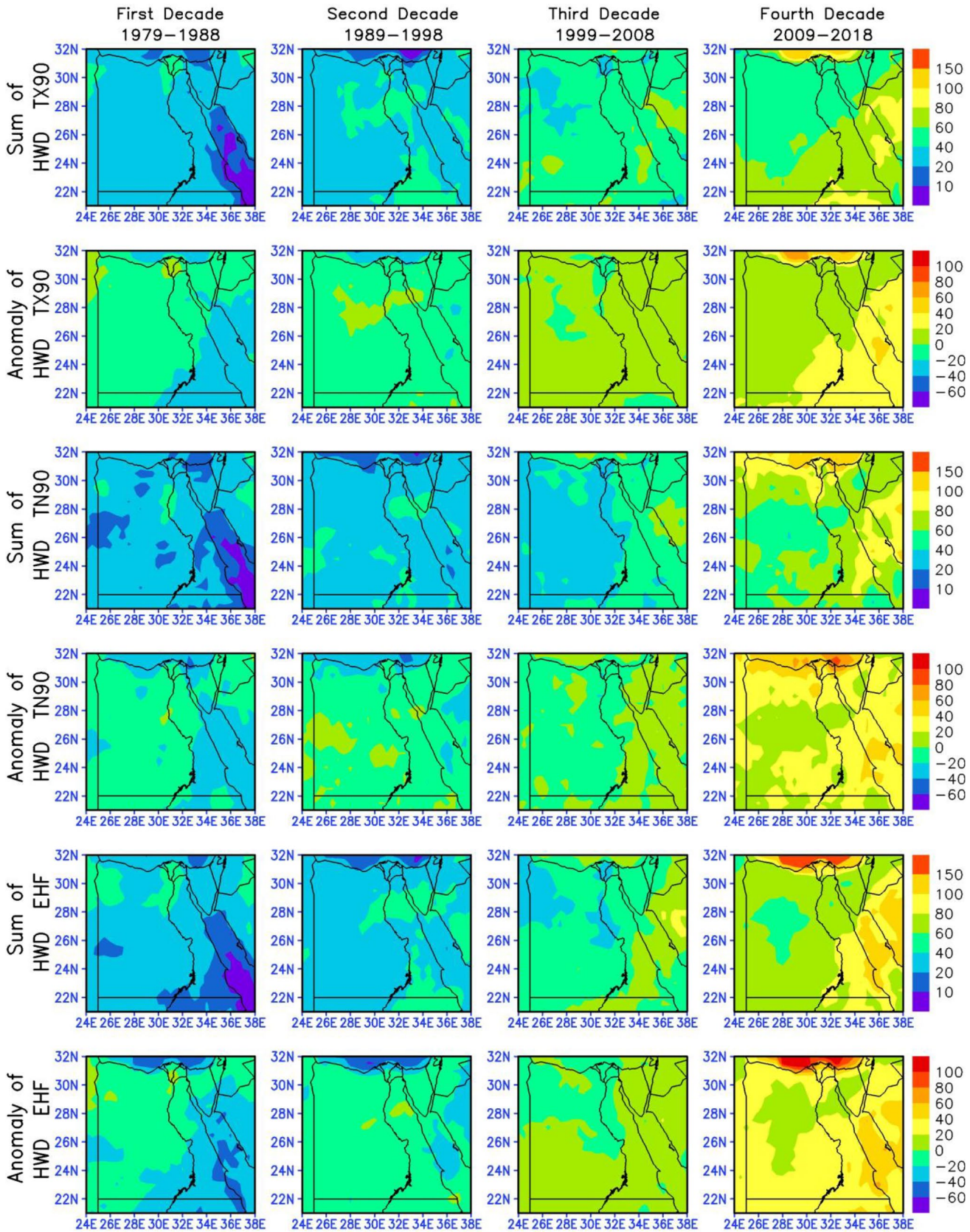
First Decade
1979–1988
Second Decade
1989–1998
Third Decade
1999–2008
Fourth Decade
2009–2018
Sum of HWD TX90
Anomaly of HWD TX90
Sum of HWD TN90
Anomaly of HWD TN90
Sum of HWD EHF
Anomaly of HWD EHF
32N
30N
28N
26N
24N
22N
24E 26E 28E 30E 32E 34E 36E 38E
150
100
80
60
40
20
10
100
80
60
40
20
0
−20
−40
−60

◂**Fig. 3** Decadal summation of the yearly heatwave duration (HWD) using TX90 (first row), TN90 (third row), and EHF (fifth row) with their anomalies (TX90 in the second row, TN90 in the fourth row, and EHF in the sixth row) from the average of their summation through the four decades

$$\text{Adjustment}(2) = \left(\frac{RH - 85}{10}\right) \times \left(\frac{87 - T}{5}\right) \quad (7)$$

This HI (Eq. (5)) with the two adjustments is not appropriate when the HI value below about 26.5 °C. In this case, a simpler HI formula is applied to obtain HI values consistent with Steadman's results:

$$HI = 0.5 \times [T + 61 + ((T - 68) \times 1.2) + (\text{RH} \times 0.094)] \quad (8)$$

Furthermore, there is a direct relationship between T and RH and HI, meaning that if T and RH increase (decrease), HI will increases (decreases). The HI severity gradient and categories based on the U.S. NWS are shown in Table 2, where exposure to full sunlight or direct sunlight will increase heat index values by up to 8.5 °C.

6 Results and discussion

6.1 Heatwave number (HWN)

Heatwave number (HWN) denotes the yearly number of HW events. The decadal summations and anomalies of HWN for the selected four consecutive decades using the three HW indexes (TX90, TN90, and EHF) are illustrated in Fig. 2. In addition, Table 3 shows the range of the decadal summations and anomalies of the yearly HWN for each decade. Based on TX90, TN90, and EHF (Fig. 2 first column and Table 3), most of Egypt has been invaded by 5–20 HW events except the Nile delta, which have greater than 20 events excluding TN90 during the first decade (1979–1988). The decadal summation of HWN increases gradually from the second to the fourth decade, where most of Egypt has been invaded by 10–30, 20–30 excluding TN90 from 10–20, and 20–45 events during the second, third, and fourth decade respectively. The decadal anomalies of HWN using TX90, TN90, and EHF (Fig. 2 second, fourth, and sixth rows respectively) indicate that there is a considerable increase in HWN with time, where the HWN anomaly from TX90, TN90, and EHF is below normal (less than Zero) over most Egypt in the first two decades (1979–1988 and 1989–1998) and still below normal in some regions during the third decade (1999–2008). The largest above normal (greater than Zero) of decadal HWN (positive anomalies) overall Egypt is occurring during the fourth decade based on the three HW indices (TX90, TN90, and EHF) as presented in Fig. 2 and Table 3. The significant increase of this HWN and its trend coincided with the projected changes of the HWN in the region of the Eastern Mediterranean and the Middle East (EMME), by Lelieveld et al. (2012) and Zittis et al. (2016). The World Meteorological Organization (2003) evaluation report also stated that the frequency and intensity of heatwaves are likely to increase with global temperatures continuing to rise due to climate change.

The yearly HWN time-latitudinal (T-Lat) cross-sections (accumulated HWN at each latitudinal grid point and each year's overall longitudinal grid points) overall Egypt (not shown) is less than 60 accumulated events during the first decade based on the three HW indices except 1988 which have HWN T-Lat greater than 60 events and reaches approximately 180 events in TX90, especially at the lower latitudes. The second decade has a small increase in HWN T-Lat than the first one, and it gradually increases during the third and fourth decades till 2015. The period from 2015 to 2018 has the greatest HWN with maximum values between 2017 and 2018.

6.2 Heatwave duration (HWD)

The length (in days) of the longest yearly HW event is defined as the heatwave duration (HWD). The decadal summations and anomalies of HWD and their ranges using the three HW definitions (TX90, TN90, and EHF) during the selected four decades are given in Fig. 3 and Table 4 respectively. The decadal summation of HWD is nearly similar for each HW index across the selected four

Table 4 The ranges of the decadal summations and anomalies of the yearly heatwave duration (HWD) for each decade using the three HW definitions (TX90, TN90, and EHF)

HWD						
Decade	Decadal summation			Anomaly		
	TX90	TN90	EHF	TX90	TN90	EHF
1979–1988	5:50	5:55	5:60	−35:5	−45:5	−50:5
1989–1998	10:65	10:50	10:60	−45:5	−45:5	−60:5
1999–2008	30:75	20:70	35:85	−12:18	−20:20	−20:20
2009–2018	40:130	40:150	60:200	0:70	10:90	10:120

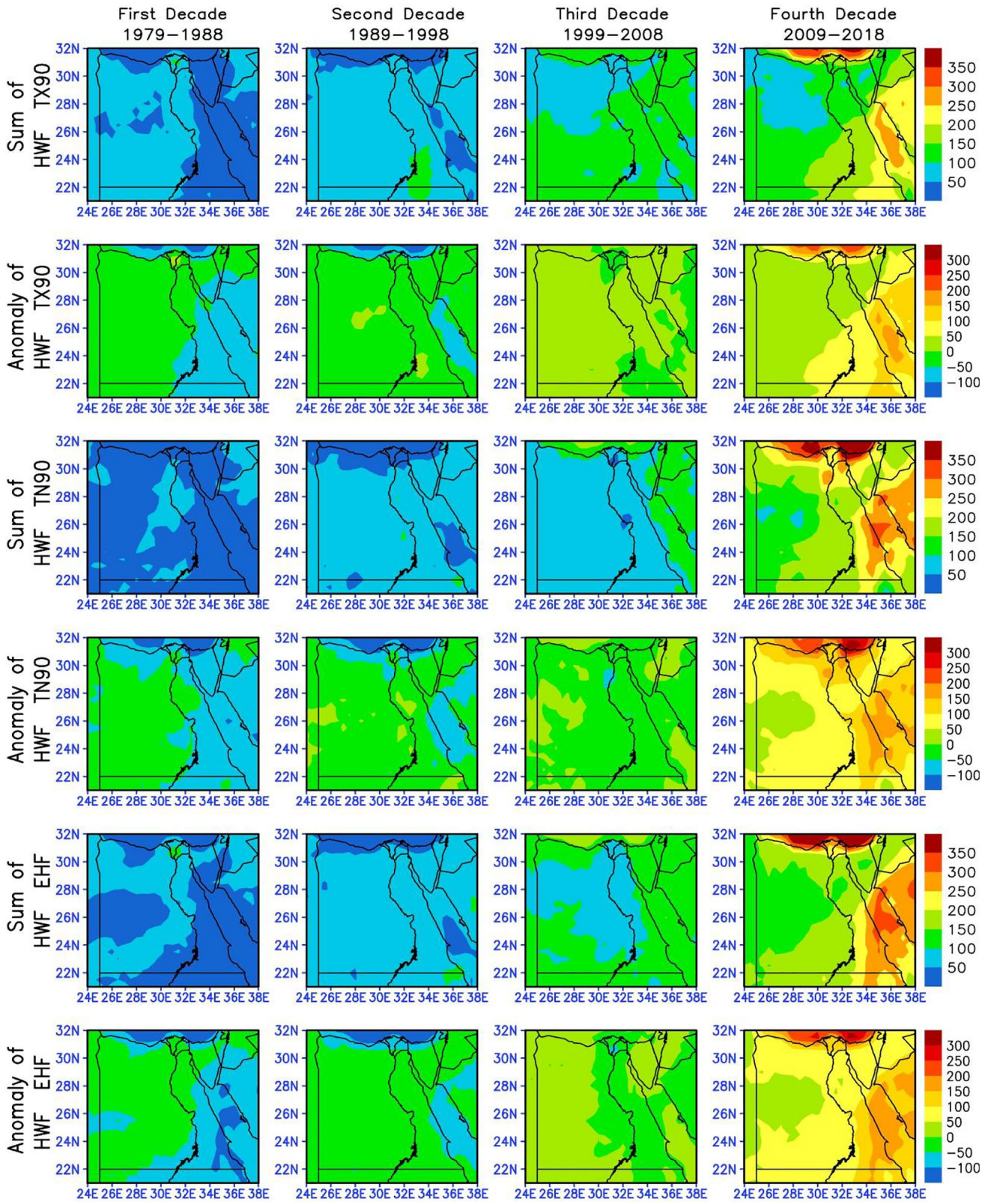

Fig. 4 Decadal summation of the yearly heatwave frequency (HWF) using TX90 (first row), TN90 (third row), and EHF (fifth row) with their anomalies (TX90 in the second row, TN90 in the fourth row, and EHF in the sixth row) from the average of their summation through the four decades

Table 5 The ranges of the decadal summations and anomalies of the yearly heatwave frequency (HWF) for each decade using the three HW definitions (TX90, TN90, and EHF)

HWF						
Decade	Decadal summation			Anomaly		
	TX90	TN90	EHF	TX90	TN90	EHF
1979–1988	10:100	20:90	20:110	− 120:10	− 150:20	− 140: − 10
1989–1998	10:110	10:130	10:120	− 130:0	− 140:20	− 140: − 20
1999–2008	70:150	40:180	60:180	− 30:40	− 60:40	− 50:40
2009–2018	60:390	100:500	150:450	0:240	30:330	− 30:300

decades. The three HW indices (TX90, TN90, and EHF in Fig. 3 first row, third row, and fifth row respectively) indicate that most of Egypt during the first two decades (Fig. 3 left column) has 20–40 accumulated HWD with below normal (negative anomalies) decadal anomaly values. It is also denoted from both Fig. 3 and Table 4 that there is a significant increase in the decadal summation and positive anomalies of HWD during the last two decades as identified by Driouech et al. (2020) over the Middle East and North Africa (MENA) region. The highest decadal summation of HWD (above 130 days) and its largest positive anomalies based on the three HW indices are detected in the last decade (2009–2018). Although the decadal summation value of HWD computed from TN90 (Fig. 3 third row) is relatively smaller than its computed value from TX90 and EHF in the second and the third decade, TN90 has greater values for both HWD decadal summation and anomalies than TX90 and still smaller than EHF in the first and fourth decade.

The T-Lat cross-section of yearly HWD (not shown) calculated from TX90, TN90, and EHF relatively behaves in a similar way to HWN T-Lat variation, where most of HWD T-Lat is less than 50 days overall Egypt during the first decade except the years 1987 and 1988 that have HWD T-Lat greater than 100 days. The HWD T-Lat gradually increases during the second and third decades, while the fourth decade except 2009 (have HWD T-Lat less than 100 days) has the maximum HWD especially in 2015 and reached above 500 days over the south, north, and all Egypt from the TX90, TN90, and EHF respectively.

6.3 Heatwave frequency (HWF)

HWF represents the summation of days per year that contribute to the HW events. The decadal summations of HWF during the selected four decades computed from TX90, TN90, and EHF are illustrated in Fig. 4 first, third, and fifth rows respectively, while the HWF decadal anomalies from the same three indices are shown in Fig. 4 second, fourth, and sixth rows respectively. And, the ranges of HWF decadal summations and anomalies are presented in Table 5. It is noticed from both Fig. 4 and Table 5 that the first decade has the smallest decadal summations and anomalies of HWF based on the three HW indices, where the smallest values indicated from TN90, EHF, and TX90 respectively. The decadal summations and the positive anomalies of HWF in the second decade followed by the third decade are relatively larger than the first decade but have the same behavior and ranking of indices (TN90, EHF, and TX90). The highest decadal summation with maximum ranges above 100 days and the positive anomaly of HWF are arising in the last decade (2009–2018), where the highest values appear from the TN90 index followed by EHF and TX90. This dramatic increase in the HWF trend matches different results over the EMME region as the ones given by Lelieveld et al. (2012) and Zittis et al. (2014).

The HWF T-Lat cross-section (not shown) is characterized by the same behavior of HWN and HWD, where the first decade has the smallest HWF, mostly less than 100 days, except for 1987–1988, which reached more than 500 days. HWF T-Lat gradually increases from the second to the third decade and reaches its maximum during the fourth decade, especially in the period from 2015 to 2018 in addition to 2010.

6.4 Heatwave amplitude (HWA)

The HWA is defined according to the applied HW index as the hottest day or night in °C in the year using TX90 or TN90 calculations, while it represents the maximum daily value of EHF in $°C^2$ through the year when using EHF. Figure 5 (first, third, and fifth rows) shows the decadal summations of HWA and their anomalies (second, fourth, and sixth rows) for each HW index (TX90, TN90, and EHF) during the selected consecutive four decades (columns from left to right). Also, the decadal summations and anomalies ranges for HWA are pointed out in Table 6. The spatial distribution of HWA decadal summations and anomalies are nearly similar to the previous three HW aspects (HWN, WHD, and HWF) obtained from the three HW indices (TX90, TN90, and EHF), where the smallest HWA decadal summations with below normal (negative anomalies) are presented in the first decade and gradually increase up to the fourth decade with above normal (positive anomalies). Therefore, the

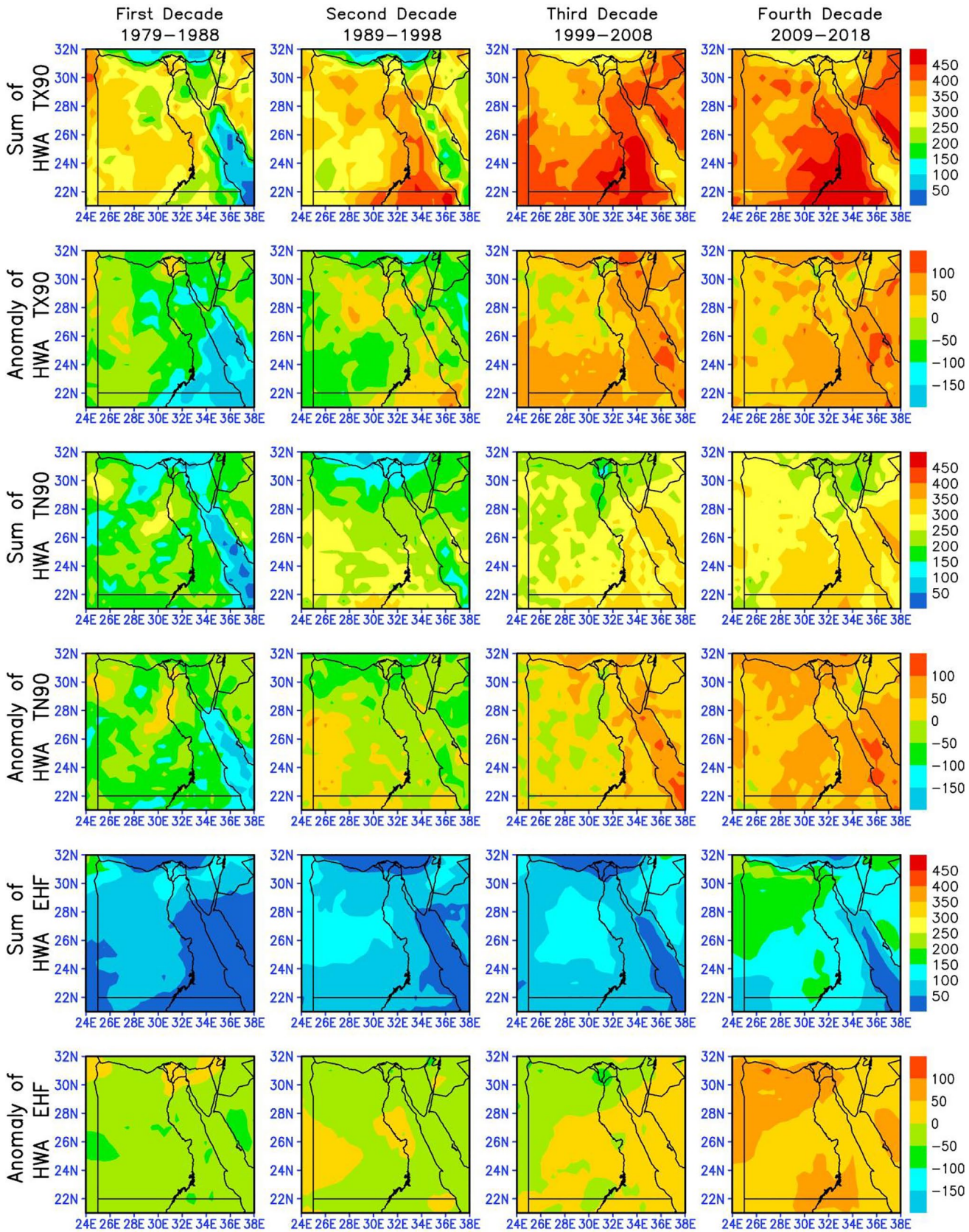
First Decade
1979–1988
Second Decade
1989–1998
Third Decade
1999–2008
Fourth Decade
2009–2018
Sum of HWA TX90
Anomaly of HWA TX90
Sum of HWA TN90
Anomaly of HWA TN90
Sum of HWA EHF
Anomaly of HWA EHF
32N
30N
28N
26N
24N
22N
24E 26E 28E 30E 32E 34E 36E 38E
450
400
350
300
250
200
150
100
50
0
−50
−100
−150

◂**Fig. 5** Decadal summation of the yearly heatwave amplitude (HWA) using TX90 (first row), TN90 (third row), and EHF (fifth row) with their anomalies (TX90 in the second row, TN90 in the fourth row, and EHF in the sixth row) from the average of their summation through the four decades

highest HWA decadal summations and positive anomalies over most of Egypt for the three indices occurred during the fourth and third decade respectively. Thus, the current results are comparable to the projected changes in HWA that given by Zittis et al. (2016) and Lelieveld et al. (2012), since the highest decadal summation and anomalies of HWA occurred in the southeast Egypt from TX90 (400 to 460 °C) and TN90 (300 to 340 °C) and are confined to the central northwest from EHF (140 up to 240°C^2) especially during the third and fourth decade. Finally, the highest HWA decadal summations are detected from the TX90 index followed by TN90 and EHF respectively.

The T-Lat cross-section of yearly HWA (not shown) has a different behavior compared to HWN, HWD, and HWF, where the highest T-Lat values as calculated from TX90 and the moderate from TN90 and the lowest from EHF; all have the same yearly increasing trend behavior. It is noticed that the lowest T-Lat values of HWA are noticed during the first decade except 1987 and 1988, while the highest values are in the last (fourth) decade from the three indices. And, the HWA T-Lat gradually increases up to the fourth decade. HWA reaches its maximum during the fourth decade except the year 2009 from the three indices.

6.5 Heatwave magnitude (HWM)

The average daily magnitude of all HW events within a year represents the annual HWM, while the total annual HWM occurs every 10 years (through the period 1979–2018) specifies the decadal summation. Figure 6 illustrates the decadal summations and anomalies of HWM, while Table 7 provides the range of decadal summations and anomalies for each HW index over the four selected decades. Like HWA behavior, HWM decadal summation and anomalies calculated from TX90 are higher than both TN90 and EHF (generates minimum values) during all decades. The lowest decadal HWM summations with mostly negative anomalies from the three HW indices are occurred in the first decade, particularly over the Red Sea and small parts of south and southeastern Egypt for TX90 (− 50 °C), TN90 (− 30 °C), and EHF (− 10°C^2).

Furthermore, the spatial patterns of HWM decadal summation and anomalies are almost like the corresponding HWA. For TX90 (Fig. 6 first row), HWM decadal summation has values above 200 °C during the first and second decades over most of Egypt, while its values mostly greater than 300 °C during the third and fourth decade. In addition, most HWM decadal anomaly values from TX90 (Fig. 6 second row) are greater than − 100 °C during the first two decades except over the Red Sea and southeastern part of Egypt in the first decade (lower than − 100 °C). For TN90 (Fig. 6 third row), HWM decadal summation values range from 60 °C to about 300 °C during the first and second decade and greater than 200 °C to above 300 °C, except Nile delta (less than 200 °C), during the third and fourth decade. Furthermore, the decadal anomalies of HWM from TN90 (Fig. 6 fourth row) are mostly negative in the first two decades except the southwestern part of Egypt in the second decade, while it is mostly positive during the last two decades. For EHF (Fig. 6 fifth row), Egypt is often covered by HWM decadal summation values below 50°C^2 over most Egypt during all decades but exceeds 50°C^2 on large spatial areas in the fourth decade compared to the first three decades. The decadal HWM anomalies from EHF has a positive value (greater than zero) in different regions during all decades with the largest spatial coverage (over 20°C^2) in the fourth decade, where the positive anomalies were detected in northwestern, central, and southeastern parts of Egypt in the first, second, and third decade respectively. The HWM T-Lat yearly cross-section (not shown) has the same behavior as HWA, where their maximum, moderate, and lowest values are obtained from TX90, TN90, and EHF respectively. The first decade has the lowest T-Lat values of HWM except 1987 and 1988, while the last decade, particularly from 2015 to 2018, has the highest values based on the three HW indices. It is also noticed that the HWM T-Lat gradually increases starting from the second to the fourth decade, while it reaches the maximum during the fourth decade except 2009 from the

Table 6 The ranges of the decadal summations and anomalies of the yearly heatwave amplitude (HWA) for each decade using the three HW definitions (TX90, TN90, and EHF)

HWA						
Decade	Decadal summation			Anomaly		
	TX90	TN90	EHF	TX90	TN90	EHF
1979–1988	50:400	60:300	20:220	− 210:30	− 180:30	− 60:40
1989–1998	100:450	60:330	10:140	− 120:120	− 100:60	− 50:20
1999–2008	260:460	100:340	20:150	− 20:100	− 40:120	− 70:40
2009–2018	240:460	180:340	20:240	− 20:120	− 40:120	10:110

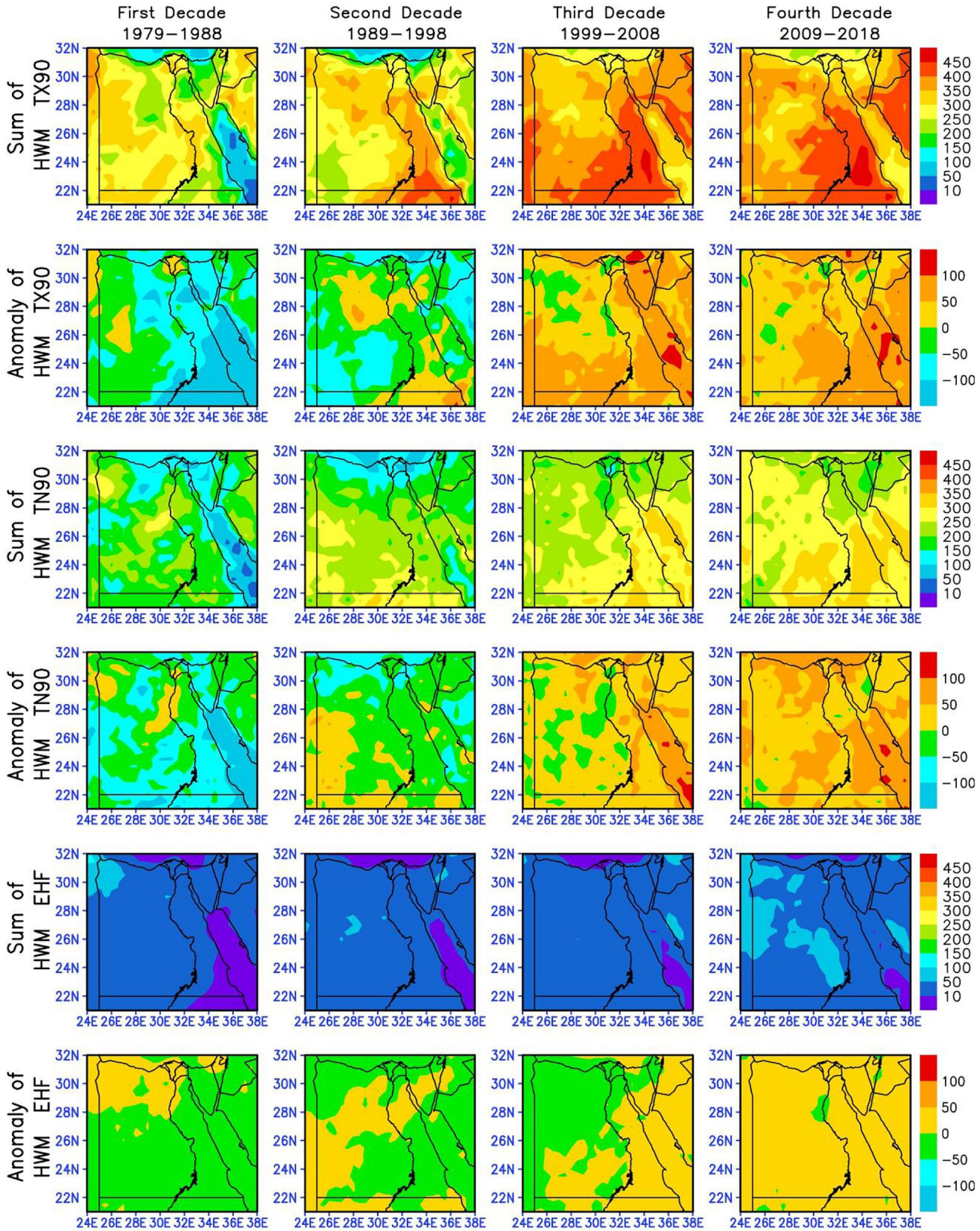

Fig. 6 Decadal summation of the yearly heatwave magnitude (HWM) using TX90 (first row), TN90 (third row), and EHF (fifth row) with their anomalies (TX90 in the second row, TN90 in the fourth row, and EHF in the sixth row) from the average of their summation through the four decades

Table 7 The ranges of the decadal summations and anomalies of the yearly heatwave magnitude (HWM) for each decade using the three HW definitions (TX90, TN90, and EHF)

HWM						
Decade	Decadal summation			Anomaly		
	TX90	TN90	EHF	TX90	TN90	EHF
1979–1988	50:400	60:270	10:110	− 210:30	− 180:40	− 20:40
1989–1998	100:450	60:300	5:55	− 120:120	− 100:60	− 20:10
1999–2008	240:440	100:320	10:70	− 30:110	− 40:120	− 25:20
2009–2018	220:440	180:320	10:75	− 20:120	− 40:120	− 3:21

three HW indices. The research conducted by Driouech et al. (2020) confirms our findings and shows that HWM is one of the main factors aggravating the MENA region heatwaves.

6.6 Heat index (HI)

It is detected that the five heatwave aspects (HWN, HWD, HWF, HWA, and HWM) have increased gradually from the first decade (1979–1988) up to the last decade (2009–2018), which means an increase in the number and intensity of heatwaves over Egypt under climate change conditions. As heatwaves have a negative and direct impact on the vital processes of the human being and his health, so investigating its real impact on humans is a very important research point. The effects of relative humidity and temperature are often combined to produce a heat index (HI) that measures a human's comfort or discomfort and assesses the effect of heatwaves on the human body and health. The decadal average and anomalies of annual averages over the Northern Hemisphere summer period (May to September) for temperature (T, °C), relative humidity (RH, %), wind speed (WS, m/s), and heat index (HI, °C) over Egypt is presented in Fig. 7. Also, Table 8 provides the decadal average and anomalies range for each parameter across the selected four decades. The spatial distribution of T and HI is relatively consistent with the spatial distribution of the five HW aspects in each decade. The decadal anomalies of T and HI have been negative (below normal) across Egypt during the first two decades and have been positive (above normal) in most regions of Egypt over the last two decades.

Furthermore, the spatial patterns of RH (Fig. 7 third row) indicate that the major humidity source over mast Egypt is the Mediterranean Sea and the minor source is the Red Sea during the summer period (May to September). Although the RH in the southern region of Egypt is lower than in the northern region, with a difference of about 30–40%, HI in the southern is greater than in the north due to the increase in temperature in the southern than in the northern by a rate of 7–10 °C. Since RH does not change (nearly remains constant) during all decades, it does not significantly influence HI changes, and thus, the temperature has the most effective role in determining HI than RH over Egypt. Most of Egypt in the first two decades falls under the influence of the caution range of HI (26–32 °C), as shown in Fig. 7 fifth row. In addition, the maximum HI values were found in the southeastern part of Egypt in all decades, but its intensity gradually increased during the last two decades, reaching extreme caution (> 32 and < 41 °C). Also, the extreme caution values of HI cover a large spatial area in southeastern Egypt during the fourth and third decades compared to the first two decades in which the HI values fall within the caution range in most of Egypt. Despite the significant increase in the five aspects of the heatwave (HWN, HWD, HWF, HWA, and HWM) and temperature (T), especially during the last two decades, environmental conditions across Egypt are more tolerable and comfortable for the human body (HI < 38), this is because RH remains constant during all decades. It is evident from Fig. 7 and Table 8 that the decadal averages of RH and wind speed (WS) are almost similar with the same spatial distribution overall for decades.

Meanwhile, a gradual increase in the decadal averages of both temperature and HI is detected from the first decade (1979–1988) until they reached their maximum values during the fourth decade (2009–2018). It is also clear that the decadal anomalies of temperature and HI have negative values in most parts of Egypt during the first two decades, while the positive values gradually increase and cover most of Egypt during the third and fourth decades. These gradual increases in both T and HI are due to global climate change which in turn leads to an increase in the number and intensity of both heatwaves and extreme events (World Meteorological Organization 2003).

The T-Lat yearly cross-section for T, RH, WS, and HI (not shown) indicates that the first decade has the lowest T-Lat values for T except for south of 23° N in 1987 and 1988 (> 32 °C), while the fourth decade, particularly in 2010 and 2015–2018, has the highest values for T (> 33 °C) south of 23° N. Also, the T-Lat values for T gradually increase on the same latitude from the second to the fourth decade, where the T-Lat results and distribution for T are almost in agreement with the T-Lat findings for the five HW aspects. Furthermore, the maximum T-Lat values for RH (> 40%) north of 30° N and the prevailing WS is between 3.2 and 3.6 m/s. Although the relative humidity values decrease with

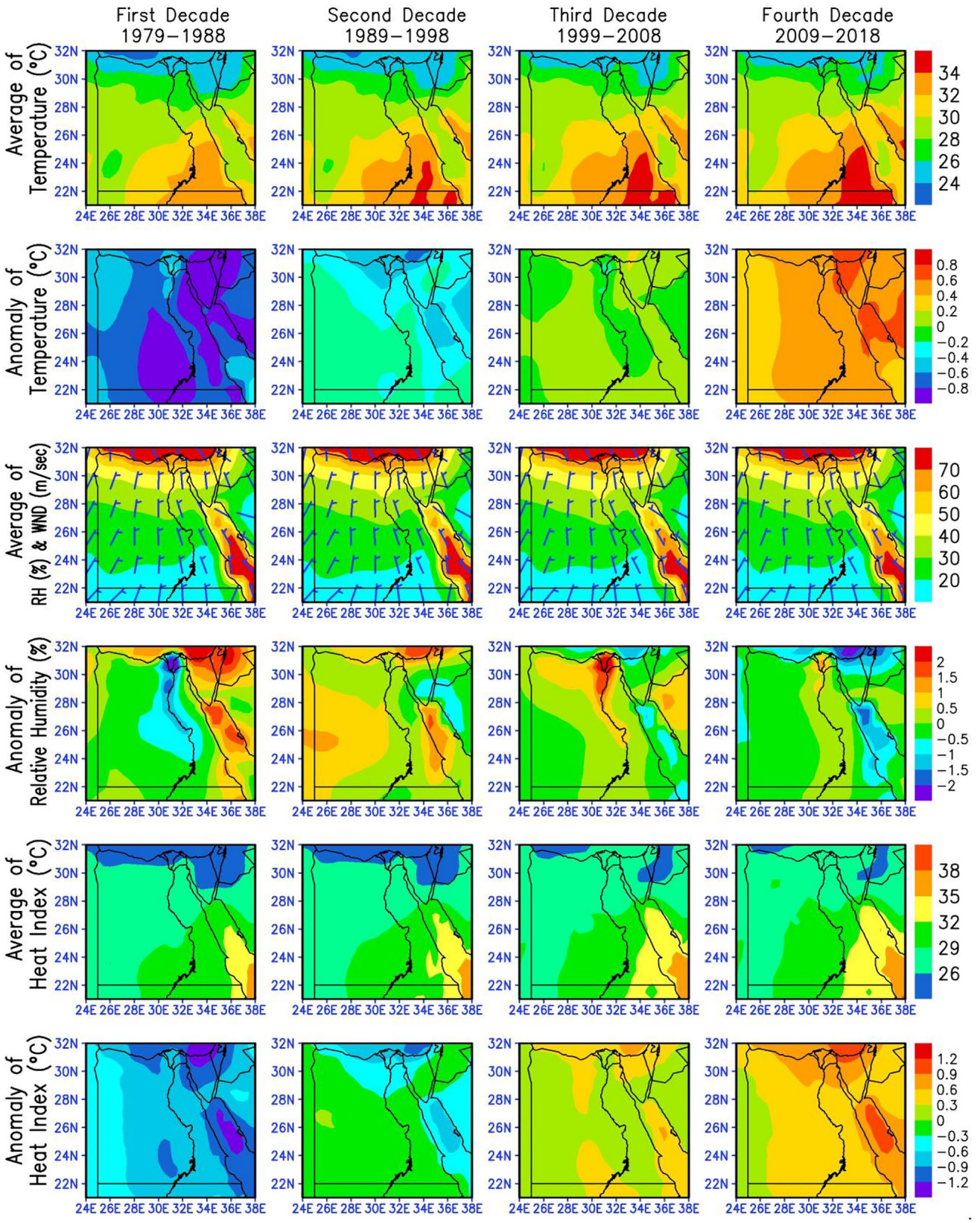

Fig. 7 Decadal average of the yearly temperature (the first row), relative humidity and wind speed (third row), and heat index (fifth row) with their anomalies (temperature in the second row, relative humidity, and wind speed in the fourth row, and heat index in the sixth row) from the average of their summation through the four decades

Table 8 The ranges of the decadal averages and anomalies of the yearly T (°C), RH (%), WS (m/s), and HI (°C)

Decade	Decadal average				Anomaly			
	T (°C)	RH (%)	WS (m/s)	HI (°C)	T (°C)	RH (%)	WS (m/s)	HI (°C)
1979–1988	24:33	20:75	1.5:5.5	24:36	−1:−0.3	−2:2.5	−0.5:0.6	−1.4:−0.5
1989–1998	24:34	20:75	1.5:5.5	25:37	−0.7:−0.1	−0.9:1.8	−0.6:0.3	−1:0
1999–2008	25:35	20:75	1.5:5.5	26:38	−0.1:0.4	−1:2.5	−0.2:0.3	0.1:0.7
2009–2018	25:35	20:75	1.5:5.5	26:38	0.4:1.2	−2:0.9	−0.4:0.5	0.4:1.8

the small gradient (20–45%) south of 30° N and increase with the higher gradient (45–70%) north of 30° N (because the main source of humidity is the Mediterranean Sea), there are no remarkable changes in the relative humidity over time. Also, the dominant WS ranged from 3.6 to 4 m/s with maximum core (> 4 m/s) around 24° N. Moreover, the largest T-Lat values for RH in middle Egypt (24–28° N) occurred during the second decade and the beginning of the third decade across the period 1990–2003. Also, the T-Lat values for HI are the lowest during all decades with caution (< 32° C) category overall Egypt except extreme caution (> 32° C) in 2010 and 2018 during the last decade. In addition, the T-Lat values for HI below 26° C were found only in the first two decades and 2000, 2004, 2005, and 2006 in the third decade north of 30° N.

7 Conclusions

This study used the existing new and superior ET-SCI percentile-based threshold indices by employing the ClimPACTv2 (R-based) software to examine, analyze, and understand the decadal changes and severity of heatwaves (HWs) over Egypt. To calculate the five HW aspects (HWN, HWD, HWF, HWA, and HWM) based on the three HW indices (TX90, TN90, and EHF), the homogenized ERA-Interim daily dataset was used, while the monthly mean dataset was used to compute the heat index (HI) during the period 1979–2018. It is recognized that the lowest decadal summations and anomalies of the five WH aspects are detected in the first decade and gradually increased to record the highest value in the last decade (particularly in 2015–2018) which was confirmed by HI.

Most of the Egyptian territory has been invaded by 5–20, 10–30, 20–30, and 20–45 events (HWN) during the first, second, third, and fourth decades respectively. The HWD was 20–40 days in the first decade, where the significant increase in decadal summations and positive anomalies is initiated from the second decade and reached the maximum (more than 130 days and about + 100 days respectively) in the fourth decade. The smallest HWF decadal summations (below 100 days) and anomalies (below + 20 days) were in the first decade and reached the highest decadal summation (above 100 days) and positive anomaly (above + 250 days) in the last decade. Based on the T-Lat cross-section, the calculation of HWN, HWD, and HWF aspects using the three HW indices is relatively similar in behavior, where TN90 provides the highest values followed by EHF and finally TX90. Although the T-Lat cross-section for HWA and HWM reveals that TX90 produces the highest values followed by TN90 and finally EHF, unlike the previous three aspects, the first decade contains the smallest decadal summations and anomalies that gradually increase until the fourth decade. The highest HWA values occurred in southeastern Egypt from TX90 (400–460 °C) and TN90 (300–340 °C) and are being confined to the northwest from EHF (140–240°C^2) during the fourth decade. HWM values exceed 300 °C, 200 °C, and 50°C^2 from TX90, TN90, and EHF respectively on large spatial areas in Egypt during the fourth decade. This significant increase in the trend of the five heatwave aspects is in agreement with the results of the projected changes in HWN, HWF, HWD, and HWA by Zittis et al. (2016) and was also identified by Lelieveld et al. (2012) and Zittis et al. (2014) over the Eastern Mediterranean and the Middle East (EMME). This increasing trend is also consistent with the results of Driouech et al. (2020) in the Middle East and North Africa, which reveals that Heatwaves are projected to intensify in terms of HWN, HWD, and HWM. Zittis et al. (2016) and Lelieveld et al. (2016) explained that these changes in heatwave peaks can be attributed to the strong summer anticyclones projected over EMME, leading to a strong advection of warm air masses from lower to the northern latitudes and more pronounced adiabatic heating. The decadal anomalies of temperature and HI have been negative during the first two decades, while they have been positive over the last two decades across Egypt. In the first two decades, most of Egypt falls within the caution range of HI (26–32 °C), where the maximum HI values were found in the southeastern part of Egypt in all decades and reaching the extreme caution (> 32 and < 41 °C) in the last two decades. Since the decadal averages of relative humidity (RH) and wind speed (WS) patterns remain nearly constant over the four decades, RH does not contribute significantly compared to temperature (which has the most effective role in determining HI) and this, in turn, creates comfortable and tolerable environmental conditions for a human body during heatwaves in Egypt. Also, the maximum RH occurred in the northern part of Egypt due to the major humidity source

from the Mediterranean Sea during the summer period (May to September).

One may conclude that there is a considerable increase in trends for all HW aspects over the selected four consecutive decades with a significant increase in the last decade (2009–2018). Therefore, the annual and the decadal occurrences of HW aspects reveal that Egypt may face local warming soon. It could lead to adverse impacts on all environmental sectors, society, and humans. Therefore, appropriate planning for decision-making for HW mitigation strategies requires further research on aspects of HW and extreme temperature in Egypt. The results of this study can provide valuable information for the various sectors that may be affected by HWs, as well as assist in the development of mitigation and adaptation strategies to HWs. The T-Lat values for HI reveal that all Egypt fall within the caution (< 32° C) category during all decades except some extreme caution (> 32° C) zones south of 24° N in 2010 and 2018 during the last decade. The maximum T-Lat values for RH (> 40%) north of 30° N and the prevailing WS is below 3.6 m/s. RH values decrease southward of 30° N and reach below 25% south of 22° N and the dominant WS above 3.6 m/s with maximum core (> 4) around 24° N. HWs usually occur in synoptic situations with pronounced slow air mass development and movement, leading to intensive and prolonged heat stress (Koppe et al. 2004).

Acknowledgements The authors would like to thank the European Centre for Medium-Range Weather Forecasts Interim (ECMWF/ERA-Interim) for providing the gridded meteorological parameters and to Expert Team on Sector-Specific Climate Indices (ET-SCI) for developing and making available the ClimPACTv2 software to compute the cores set of their defined climate-related.

Author contributions All authors contributed to the study conception, Idea, and design. Material preparation, data collection and analysis, and discussion of results were performed by all authors. The first draft of the manuscript was written and prepared by all authors. All authors commented on previous versions of the manuscript. All authors read and approved the final manuscript.

Data availability The data supporting the findings of this article is included within the article.

Code availability The ClimPACTv2 software is used to calculate the five heatwave aspects.

Declarations

Ethics approval Not applicable.

Consent to participate Not applicable.

Consent for publication Not applicable.

Conflict of interest The authors declare no competing interests.

References

Abatan AA, Abiodun BJ, Lawalc KA, Gutowski WJ (2016) Trends in extreme temperature over Nigeria from percentile-based threshold indices. Int J Climatol 36:2527–2540. https://doi.org/10.1002/joc.4510

Abdel Basset H, Hasanen HM (2006) Heat wave over Egypt during the summer of 1998. Int J Meteorol 31(308):133–145

Aboelkhair H, Morsy M, El Afandi G (2019) Assessment of agroclimatology NASA POWER reanalysis datasets for temperature types and relative humidity at 2 m against ground observations over Egypt. Adv Space Res 64(1):129–142. https://doi.org/10.1016/j.asr.2019.03.032

Alexander LV, Herold N (2015) ClimPACTv2 indices and software. WMO Commission for Climatology Expert Team on Sector-Specific Climate Indices. Accessed 19 Feb 2016. https://github.com/ARCCSS-extremes/climpact2

Alghamdi AS, Harrington J Jr (2018) Time-sensitive analysis of a warming climate on heat waves in Saudi Arabia: temporal patterns and trends. Int J Climatol 38:3123–3139. https://doi.org/10.1002/joc.5489

Andersen OB, Seneviratne SI, Hinderer J, Viterbo P (2005) GRACE-derived terrestrial waterstorage depletion associated with the 2003 European heat wave. Geophys Res Lett 32:L18405. https://doi.org/10.1029/2005GL023574

Añel J, Fernández-González M, Labandeira X, López-Otero X, Torre L (2017) Impact of cold waves and heatwaves on the energy production sector. Atmosphere 8:209. https://doi.org/10.3390/atmos8110209

Athar H (2014) Trends in observed extreme climate indices in Saudi Arabia during 1979–2008. Int J Climatol 34:1561–1574

Baldi M, Dalu G, Maracchi G, Pasqui M, Cesarone F (2006) Heat waves in the Mediterranean: a local feature or a larger scale effect. Int J Climatol 26:1477–1487

Barriopedro D, Fischer EM, Luterbacher J, Trigo RM, Garcia-Herrera R (2011) The hot summer of 2010: Redrawing the temperature record map of Europe. Science 332:220–224. https://doi.org/10.1126/science.1201224

Chen Y, Hu Q, Yang Y, Qian W (2017) Anomaly based analysis of extreme heat waves in Eastern China during 1981–2013. Int J Climatol 37:509–523. https://doi.org/10.1002/joc.4724

Coumou D, Rahmstorf S (2012) A decade of weather extremes. Nat Clim Chang 2:491–496. https://doi.org/10.1038/nclimate1452

Dee DP, Uppala SM, Simmons AJ, Berrisford P, Poli P, Kobayashi S, Andrae U, Balmaseda MA, Balsamo G, Bauer P et al (2011) The ERA-interim reanalysis: configuration and performance of the data assimilation system. Q J R Meteorol Soc 137:553–597

Dole R, Hoerling M, Perlwitz J, Eischeid J, Pegion P, Zhang T, Quan X-W, Xu T, Murray D (2011) Was there a basis for anticipating the 2010 Russian heat wave? Geophys Res Lett 38:L06702. https://doi.org/10.1029/2010GL046582

Domroes M, El-Tantaw A (2005) Recent temporal and spatial temperature changes in Egypt. Int J Climatol 25:51–63. https://doi.org/10.1002/joc.1114

Donat MG, Peterson TC, Brunet M, King AD et al (2014) Changes in extreme temperature and precipitation in the Arab region: long-term trends and variability related to ENSO and NAO. Int J Climatol 34:581–592

Efthymiadis D, Goodess CM, Jones PD (2011) Trends in Mediterranean gridded temperature extremes and largescale circulation influences. Nat Hazard 11:2199–2214

El Afandi G, Morsy M, El Hussieny F (2013) Heavy rainfall simulation over Sinai Peninsula using the weather research and forecasting model. Int J Atmos Sci 2013:11. https://doi.org/10.1155/2013/241050

El Ashmawy FM (2015) Study of extreme weather events over Egypt during the period from 1970 to 2010. Doctoral Thesis, Al-Azhar University, pp 153

El Kenawy AM, Hereher ME, Robaa SM (2019a) An assessment of the accuracy of MODIS land surface temperature over Egypt using ground-based measurements. Remote Sens 11(20):2369. https://doi.org/10.3390/rs11202369

El Kenawy AM, Lopez-Moreno JI, McCabe MF, Robaa SM, Domínguez-Castro F, Peña-Gallardo M, Trigo RM, Hereher ME, Al-Awadhi T, Vicente-Serrano SM (2019b) Daily temperature extremes over Egypt: spatial patterns, temporal trends, and driving forces. Atmos Res 226:219–239

Erlat E, Türkes M (2013) Observed changes and trends in numbers of summer and tropical days and the 2010 hot summer in Turkey. Int J Climatol 33:1898–1908

Fink AH, Bruecher T, Leckebusch GC, Krueger A, Pinto JG, Ulbrich U (2004) The 2003 European summer heatwaves and drought-synopstic diagnosis and impacts. Weather 59:209–216

Fischer EM, Schar S (2010) Consistent geographical patterns of changes in high-impact European heatwaves. Nat Geosci 3:398–403. https://doi.org/10.1038/ngeo866

Fontaine B, Janicot S, Monerie P-A (2013) Recent changes in air temperature heat waves occurrences and atmospheric circulation in Northern Africa. J Geophys Res Atmos 118:8536–8552. https://doi.org/10.1002/jgrd.50667

Gamal G (2017) Future analysis of extreme temperature indices for Sinai Peninsula-Egypt. Imp J Interdiscip Res 3(1):1960–1966

Hasanean HM (2004) Wintertime surface temperature in Egypt in relation to the associated atmospheric circulation. Int J Climatol 24:985–999. https://doi.org/10.1002/joc.1043

Hasanean HM, Abdel Basset H (2006) Variability of summer temperature over Egypt. Int J Climatol 26:1619–1634. https://doi.org/10.1002/joc.1321

Hussein MMA, Mohamed EEE (2016) Temperature trend over Nile Delta Egypt in 20th century. Adv Res 7(2):1–14

IPCC (Intergovernmental Panel on Climate Change) (2013) Climate Change 2013: The Physical Science Basis Contribution of Working Group I to the Fifth Assessment Report of the Intergovernmental Panel on Climate Change, Cambridge, United Kingdom.

Kent ST, McClure LA, Zaitchik BF, Smith TT, Gohlke JM (2014) Heat waves and health outcomes in Alabama (USA): the importance of heat wave definition. Environ Health Perspect 122:151–158. https://doi.org/10.1289/ehp.1307262

Khalil AA, Hassanein MK (2016) Extreme weather events and negative impacts on Egyptian agriculture. Int J Adv Res 4(12):1843–1851. https://doi.org/10.21474/IJAR01/2592

Kim DW, Deo RC, Chung JH, Lee JS (2016) Projection of heatwave mortality related to climate change in Korea. Nat Hazards 80:623–637. https://doi.org/10.1007/s11069-015-1987-0

Klein Tank AMG, Konnen GP (2003) Trends in indices of daily temperature and precipitation extremes in Europe 1946–1999. J Clim 16:3665–3680

Koppe C, Kovats S, Jendritzky G, Menne B (2004) Heat-waves: risks and responses. Health and global environmental change series, No. 2, 123 pages. World Health Organization, Geneva, Switzerland, 2004. https://www.euro.who.int/__data/assets/pdf_file/0008/96965/E82629.pdf

Kostopoulou E, Jones PD (2005) Assessment of climate extremes in the Eastern Mediterranean. Meteorol Atmos Phys 89:69–85

Kostopoulou E, Giannakopoulos C, Hatzaki M, Karali A, Hadjinicolaou P, Lelieveld J, Lange MA (2014) Spatiotemporal patterns of recent and future climate extremes in the eastern Mediterranean and Middle East region. Nat Hazard 14:1565–1577

Kousari MR, Ahani H, Hendi-zadeh R (2013) Temporal and spatial trend detection of maximum air temperature in Iran during 1960–2005. Global Planet Chang 111:97–110

Kuglitsch FG, Toreti A, Xoplaki E, Della-Marta PM, Zerefos CS, Türkes M, Luterbacher J (2010) Heat wave changes in the eastern Mediterranean since 1960. Geophys Res Lett 37:L04802. https://doi.org/10.1029/2009GL041841

Lasheen MA (2000) on formation of summer stability condition over east Mediterranean. Al-Azhar Bulletin of Science 11(2):1–14

Lelieveld J, Hadjinicolaou P, Kostopoulou E, Chenoweth J, El Maayar M, Giannakopoulos C, Hannides C, Lange MA, Tanarhte M, Tyrlis E, Xoplaki E (2012) Climate change and impacts in the Eastern Mediterranean and the Middle East. Clim Chang 114:667–687

Lelieveld J, Proestos Y, Hadjinicolaou P, Tanarhte M, Tyrlis E, Zittis G (2016) Strongly increasing heat extremes in the Middle East and North Africa (MENA) in the 21st century. Clim Change 137(1–2):245–260. https://doi.org/10.1007/s10584-016-1665-6

Lesk C, Rowhani P, Ramankutty N (2016) Influence of extreme weather disasters on global crop production. Nature 529:84–87

Mcgree S, Herold N, Alexander L, Schreider S, Kuleshov Y, Ene E, Finaulahi S, Inape K, Mackenzie B, Malala H, Ngari A, Prakash B, Tahani L (2019) Recent changes in mean and extreme temperature and precipitation in the Western Pacific Islands. J Clim 32:4919–4941

Muslih KD, Błażejczyk K (2017) The inter-annual variations and the long-term trends of monthly air temperatures in Iraq over the period 1941–2013. Theoret Appl Climatol 130:583–596. https://doi.org/10.1007/s00704-016-1915-6

Nairn J, Fawcett R (2013) Defining heatwaves: heatwave defined as a heat-impact event servicing all community and business sectors in Australia. CAWCR technical report.

Nairn JR, Fawcett RJB (2015) The excess heat factor: a metric for heatwave intensity and its use in Understanding classifying heatwave severity. Int J Environ Res Public Health 12:227–253. https://doi.org/10.3390/ijerph120100227

Nairn J, Fawcett R, Ray D (2009) Defining and predicting excessive heat events a national system high impact weather, CAWCR modelling workshop 017: 83-86

Nashwan MS, Shahid S, Abd Rahim N (2018) Unidirectional trends in annual and seasonal climate and extremes in Egypt. Theoret Appl Climatol 136(1–2):457–473. https://doi.org/10.1007/s00704-018-2498-1

Önol B, Bozkurt D, Turuncoglu UU, Sen OL, Dalfes HN (2014) Evaluation of the twenty-first century RCM simulations driven by multiple GCMs over the Eastern Mediterranean-Black Sea region. Clim Dyn 42:1949–1965

Ozturk T, Ceber ZP, Türkeş M, Kurnaz ML (2015) Projections of climate change in the Mediterranean Basin by using downscaled global climate model outputs. Int J Climatol 35(14):4276–4292. https://doi.org/10.1002/joc.4285

Perkins SE (2011) Biases and model agreement in projections of climate extremes over the tropical Pacific. Earth Interactions 15(24):1–36. Available online at http://EarthInteractionsorg

Perkins SE, Alexander LV (2013) On the measurement of heat waves. J Clim 26:4500–4517

Perkins SE, Alexander LV, Nairn JR (2012) Increasing frequency intensity and duration of observed global heatwaves and warm spells. Geophys Res Lett 39(20):L20714

Peterson TC, Easterling DR, Karl TR, Groisman P, Nicholls N, Plummer N, Torok S, Auer I, Boehm R, Gullett D, Vincent L, Heino R, Tuomenvirta H, Mestre O, Szentimrey T, Salinger J, Førland EJ, Hanssen-Bauer I, Alexandersson H, Jones P, Parker D (1998) Homogeneity adjustments of in situ atmospheric climate data: a review. Int J Climatol 18(13):1493–1517

Piticar A, Croitoru AE, Ciupertea FA, Harpa GV (2018) Recent changes in heat waves and cold waves detected based on excess heat factor and excess cold factor in Romania. Int J Climatol 38(2):1777–1793. https://doi.org/10.1002/joc5295

Ragatoa DS, Ogunjobi KO, Klutse NAB, Okhimamhe AA, Eichie JO (2019) A change comparison of heat wave aspects in climatic zones of Nigeria. Environ Earth Sci 78:111. https://doi.org/10.1007/s12665-019-8112-8

Rothfusz LP (1990) The heat index ''equation'' (or, more than you ever wanted to know about heat index). National Oceanic and Atmospheric Administration, National Weather Service, Office of Meteorology, Southern Region Tech. Attachment SR-9023, Fort Worth, Texas, 2 pp. http://www.srh.noaa.gov/images/ffc/pdf/ta_htindx.PDF

Russo S, Dosio A, Graversen RG, Sillmann J, Carrao H, Dunbar MB, Vogt JV (2014) Magnitude of extreme heat waves in present climate and their projection in a warming world. J Geophys Res Atmoss 119(22):500–512. https://doi.org/10.1002/2014JD022098

Said MA, El-Geziry TM, Radwan AA (2012) Long-term trends of extreme climate events over Alexandria Region Egypt. INOC-CNRS International Conference on "Land-Sea Interactions in the Coastal Zone" Jounieh – LEBANON, 06–08 November: 286–293

Saleh SM, Heggi MAM, Abdrabbo MAA, Farag AA (2017) Heat waves investigation during last decades in some climatic regions in Egypt Egypt. J Agric Res 95(2):863–889

Shaposhnikov D, Revich B, Bellander T, Bedada GB, Bottai M, Kharkova T, Kvasha E, Lezina E, Lind T, Semutnikova E, Pershagen G (2014) Mortality related to air pollution with the Moscow heat wave and wildfire of 2010. Epidemiology 25(3):359–364. https://doi.org/10.1097/EDE.0000000000000090

Sillmann J, Kharin VV, Zwiers FW, Zhang X, Bronaugh D (2013) Climate extremes indices in the CMIP5multimodel ensemble: part 2 Future climate projections. J Geophys Res Atmos 118:2473–2493. https://doi.org/10.1002/jgrd50188

Smith TT, Zaitchik BF, Gohlke JM (2013) Heat waves in the United States: definitions patterns and trends. Clim Change 118:811–825

Souch C, Grimmond CSB (2004) Applied climatology: heat waves. Phys Geogr 28:599–606

Spinoni J, Lakatos M, Szentimrey T, Bihari Z, Szalai S, Vogt J, Antofie T (2015) Heat and cold waves trends in Carpathian region from 1961 to 2010. Int J Climatol 35:4197–4209. https://doi.org/10.1002/joc4279

Steadman RG (1979) The assessment of sultriness. Part I: a temperature-humidity index based on human physiology and clothing science. J Appl Meteorol 18(7):861–873. https://doi.org/10.1175/1520-0450(1979)018%3c0861:taospi%3e2.0.co;2

Stott PA, Stone DA, Allen MR (2004) Human contribution to the European heatwave of 2003. Nature 432:610–614

Tanarhte M, Hadjinicolaou P, Lelieveld J (2015) Heat wave characteristics in the Eastern Mediterranean and Middle East using extreme value theory. Clim Res 63:99–113. https://doi.org/10.3354/cr01285

Tayanç M, Im U, Dogruel M, Karaca M (2009) Climate change in Turkey for the last half century. Clim Chang 94:483–502

Wang Y, Shi L, Zanobetti A, Schwartz JD (2016) Estimating and projecting the effect of cold waves on mortality in 209 US cities. Environ Int 94:141–149

WHO (World Health Organization) (2010) Wildfires and Heat-Wave in the Russian Federation - Public Health Advice. WHO, Copenhagen, Denmark, pp 17. Retrieved from www.euro.who.int/__data/assets/pdf_file/ 0012/120090/190810_EN_Russia_wildfire_ advisory.pdf. Accessed 4 May 2011

World Meteorological Organization (2003) Extreme weather events may increase, Press Release 695, 2 July 2003, Geneva. Accessed 29 Oct 2003. http://www.wmo.ch/web/Press/Press695.doc. 318 LAREEF ZUBAIR.

Zampieri M, Russo S, di Sabatino S, Michetti M, Scoccimarro E, Gualdi S (2016) Global assessment of heat wave magnitudes from 1901–2010 and implications for the river discharge of the Alps. Sci Total Environ 571:1330–1339

Zhang X, Aguilar E, Sensoy S, Melkonyan H et al (2005) Trends in Middle East climate extreme indices from 1950 to 2003. J Geophys Res 110:D22104. https://doi.org/10.1029/2005JD006181

Zittis G, Hadjinicolaou P, Lelieveld J (2014) Role of soil moisture in the amplification of climate warming in the Eastern Mediterranean and the Middle East. Clim Res 59:27–37

Zittis G, Hadjinicolaou P, Fnais M, Lelieveld J (2016) Projected changes in heat wave characteristics in the eastern Mediterranean and the Middle East. Reg Environ Chang 16:1863–1876